A ferrite-filled cavity resonator for electronic article surveillance on metallic packaging

P.S. Keatley, E.R. Glover, B. Tremain, I.R. Hooper, A.P. Hibbins, and R.J. Hicken

Department of Physics and Astronomy, University of Exeter, Stocker Road, EXETER, EX4 4QL, UK

Abstract

Conventional electronic article surveillance (EAS) tags are ineffective on metallic packaging. The component of RF magnetic field perpendicular to the surface of the packaging induces eddy currents that suppress the magnetic flux linking the inductive element of the tag. In this work an inductive quarter-wavelength planar cavity, formed by wrapping aluminum foil around a ferrite core, was extended by wrapping additional capacitive layers of foil/dielectric around the ferrite-filled central region. This so-called 'wrapped tag' exhibits the frequency, *Q*-factor, and read distance characteristics of existing EAS tags, but is instead driven by RF magnetic fields parallel to the surface of the metallic packaging. In this article we compare the observed frequency response of the wrapped tag with a simple *LC*-resonator model that takes account of the tag's geometrical features, and use the model to describe how the design and construction of the tag can be optimized. Finite element method modeling is used to reveal how the current flows in the wrapped foil of the tag. Prototype tags show good reproducibility, demonstrating the potential of the design as a solution to the problem of tagging metallic packaging in the EAS industry.

Introduction

Microwave cavity resonators are a key component of electromagnetic technology that enjoy ubiquitous use[1], from high power microwave sources[2] and exotic particle detectors[3], to filters and absorbers[4] of microwave radiation. The challenge for everyday technology is to construct resonators in compact formats with dimensions that are small compared to the free space wavelength. A planar cavity can be defined from a pair of infinite parallel conducting planes separated by an insulator that can support a transverse electromagnetic (TEM) mode with no low frequency cut off [5]. The planes can be truncated to form a one-dimensional cavity with infinite width, and length that is much greater than the separation of the planes. The cavity can support a standing wave resonance of the TEM mode, with electric field antinodes at the open ends of the cavity, when its length is equal to a half-integer multiple of the mode wavelength [6]. If the planes are electrically connected at one end of the cavity, the electric field exhibits a node at the closed end [7, 8]. Such a cavity can support a quarter-wavelength mode and is analogous to an organ pipe cavity.

Previously it was reported that ferrite-filled quarter-wavelength cavities can act as compact planar resonators that have potential for use in electronic article surveillance (EAS) applications [9]. EAS tags are typically used to alert retailers to the unauthorized removal of goods from their premises. It is usually necessary for such tags to be discreet, covering only a small area of the product and having a low profile on its surface. It was shown that for a given frequency, and similar cavity width and thickness, the use of a ferrite filling material allowed the length of a planar cavity resonator to be reduced to approximately one quarter of the length of a similar cavity filled with Teflon. However, the frequency of the ferrite-filled cavity of $\sim 10^2$ MHz still far exceeded that required for EAS at 8.2 MHz. In the present work it is shown how such a cavity can be modified to yield a discreet, low profile tag that operates at 8.2 MHz on conducting materials. This much lower frequency was achieved by extending the length of the cavity with a thin dielectric-filled section that could then be wrapped around the shorter ferrite-filled section. The dielectric-filled section increases the capacitance of the structure. The use of a ferrite with high permeability and low loss enhances the self-inductance and quality factor so that coupling to the magnetic field from an EAS gate system is comparable to that of existing EAS tags.

Existing commercial 8.2 MHz EAS tags consist of an air core coil inductor and a capacitor connected in series to form an *LC*-resonator. The cross-sectional area of the inductor must be sufficiently large as to ensure adequate sensitivity for detection at the desired read distance. The capacitance is then chosen to achieve a frequency of 8.2 MHz. Such a tag can be readily constructed using a 5-turn cylindrical wire coil with 65 mm diameter in series with a 120 pF ceramic capacitor, Figure 1(a).

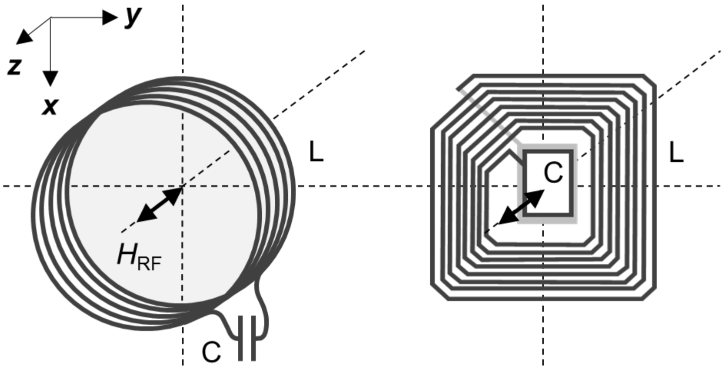

Figure 1. (a) A hard tag constructed from a wire coil inductor in series with a capacitor. (b) A deactivatable label tag constructed from a planar spiral inductor in series with a thin film capacitor.

The coil and capacitor of these so-called ‘hard tags’ results in a bulky tag that cannot be deactivated, and which must therefore be removed at the point of sale. More discreet adhesive ‘label tags’, e.g. [10], instead consist of an etched Al planar spiral inductor on a polyester substrate that surrounds a deactivatable thin film capacitor formed from a thinned region of the polyester with an Al electrode on either side, Figure 1(b). These disposable tags can be deactivated at the point of sale, by inducing a short-circuit between the plates of the capacitor and can remain on the product after purchase.

In both tags, the inductor couples to the RF magnetic field component parallel to the axis of the coil within the hard tags or the surface normal of the label tags, as shown in Figure 1. When placed onto a product this RF field component is therefore perpendicular to the material onto which the tag is placed. When the material is conducting or polarizable, the perpendicular RF field component generates eddy currents within the material that, due to Lenz’s law, generate an opposing RF field that prevents efficient excitation of the tag. The cavity-based tag presented in this work instead couples to the RF field component that lies within the plane of the material onto which it is placed, and is immune to the formation of eddy currents within the material. This design opens up the potential for discrete EAS tagging solutions for metallic or polarizable materials that could be applied to hard, or deactivatable tagging applications. It will be shown that the quarter-wavelength planar cavity can also be described by a simple *LC*-resonator model that takes account of the geometrical features of the tag, and that the geometry can be modified to yield the necessary values of *L* and *C* for operation at 8.2 MHz. The dependence of the tag frequency and linewidth on the geometry and the properties of the ferrite filling material are discussed, while finite element method modeling is used to reveal the electromagnetic field profile within the cavity and the corresponding current distribution within the metallic foil. Finally, the characteristics of the planar cavity tag, optimized for operation on a conducting material at 8.2 MHz, are presented and compared to commercially available adhesive label tags that are unable to operate on such materials.

Tag details and experimental technique

Prototype tags were formed from a closed-end cavity that consisted of a metal foil with thickness of 50 μm wrapped around three surfaces of a ferrite slab, Figure 2(a). The NiZn high frequency ferrite (MagDev F16), is specified by the manufacturer for application frequencies between 0.5 and 10 MHz. Once the ferrite-filled part of the cavity was formed, a number, *n*, of additional foil wraps were made using the same strip of foil, as indicated by the block arrow in Figure 2(a). To prevent electrical contact between the additional wraps and the foil of the ferrite-filled part of the cavity, a separate polyethylene terephthalate (PET) dielectric film with a thickness 25 μm, and width slightly larger than the foil, was inserted at the beginning of the first additional wrap, Figure 2 (a-b). The dielectric film and metal foil were then wrapped about the cavity concurrently to form the so-called 'wrapped tag', Figure 2(c). Wrapping in such a way makes a top layer of foil on the dielectric film (shown as dashed layer in Figure 2(a)) redundant once wrapped back onto itself, and so it was omitted to simplify the tag construction, yielding a structure similar to the metafilm described in reference [11]. The foil on either side of the dielectric film forms an extension of the cavity with large capacitance, while the first foil loop around the ferrite core has large inductance. The tag can either be described as an *LC*-resonator [7, 11], or as a structured quarter-wavelength cavity with a substantial change of cross-section along its length (similar to the half-wavelength cavity designs of reference [12]).

Tags were excited by a uniform radio-frequency (RF) magnetic field that was applied perpendicular to the cross-sectional area of the cavity tag, or perpendicular to the planar spiral inductor of label tags. The RF-field was generated by a single rectangular antenna loop that mimicked those of security gates used to detect EAS tags in the doorways of retail stores, Figure 2(d). A vector network analyser (VNA) was used to drive a RF current around the loop with an output power of 0 dBm and frequency swept in the range from 5 MHz to 50 MHz. The frequency, linewidth, and absorption of the RF response of the tags was extracted from the reflected power spectrum of the antenna loop recorded by the VNA, i.e. a single-port measurement of the scattering matrix element S_{11}. When the RF frequency was swept through the resonance frequency of the tag, a Lorentzian-shaped dip was observed in the power spectrum of the antenna loop corresponding to the tag resonance.

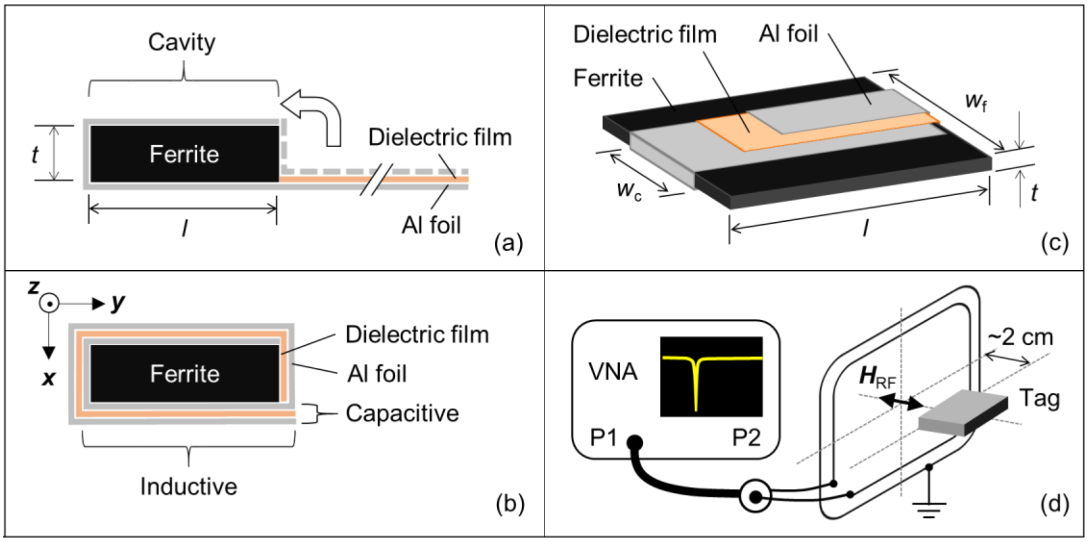

Figure 2. (a) The unwrapped construction of the tag consists of a ferrite-filled foil cavity section of length *l* and thickness *t* and an additional cavity section that is filled with a thin dielectric spacer. Foil on top of the dielectric (dashed grey) becomes redundant once wrapped back onto the cavity and is therefore removed. (b) The wrapped tag consisting of the inductive ferrite-filled part of the cavity extended by a single capacitive wrap. (c) A cut-away schematic of the tag showing the width of the ferrite core w_f, and the cavity w_c. (d) Schematic of the single port vector network analyzer (VNA) set-up used to measure the tag absorption spectra as the frequency of the excitation magnetic field $\boldsymbol{H}_{RF}$ was swept. The tag was typically placed 2 cm from the plane of the antenna loop.

To demonstrate the problem of tagging metallic packaging using label tags, VNA measurements of the tag resonance spectrum were performed for tag-packaging separation ranging from 0 to 15 cm. Figure 3(b) shows that the tag should be separated by at least 5 cm from the packaging to recover the required frequency, linewidth, and absorption for normal operation, Figure 3(a-d). Spacing the tag by such a distance (greater than the tag lateral size) would be an undesirably bulky solution. Alternatively, the use of a high permeability ferrite block (MagDev F16 with initial μ_r ~100, $l \times w_f \times t$ = 50×30×3 mm^3) between the tag and packaging can significantly reduce the tag detuning when closer than 5 cm, Figure 3(b-d). However, the high permeability modifies the tag inductance and detunes the tag to ~6.6 MHz, and so the planar spiral inductor must be redesigned to compensate for the frequency shift when placed onto ferrite limiting the use of such tags to only metal packaging. Placing the ferrite backed label tag onto the metallic surface produces negligible absorption. Surprisingly, the absorption remains reduced compared to that of the free standing label tag even as the separation from the metal surface is increased. In contrast, the integration of the same ferrite block into the design of the wrapped cavity tag, and the addition of a thin metallic shield to the outside of the tag, leads to a more effective solution for a universal tag that can be used on metallic, and non-metallic packaging. It will be shown that such a wrapped tag exhibits greater absorption on metal to that of the label tag in free space.

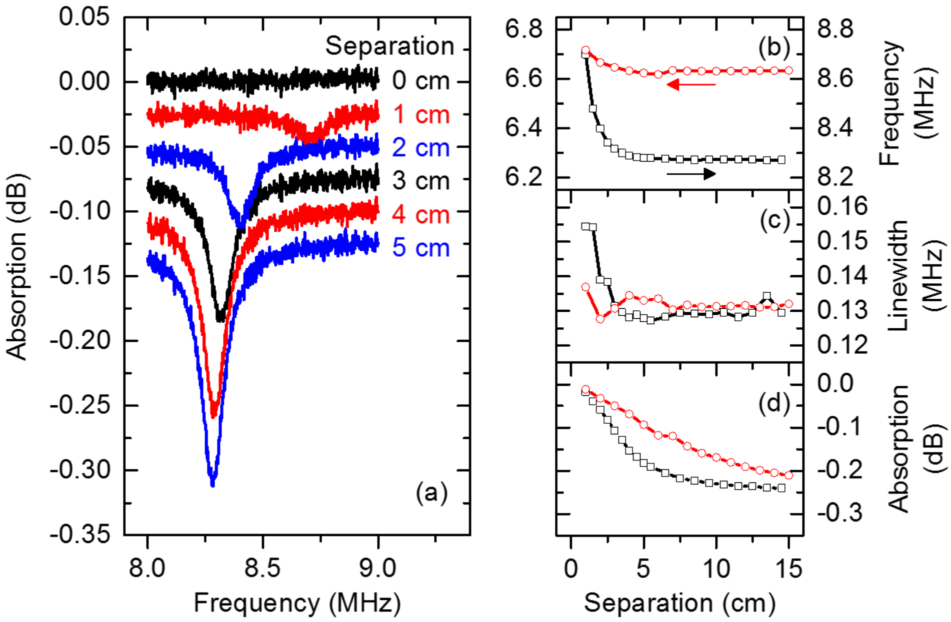

Figure 3. (a) VNA spectra acquired for the label tag only (in free space) when placed between 0 and 5 cm from the surface of metallic packaging. The tag was placed at the centre of the antenna loop in a plane parallel to that of the packaging surface. The packaging was then moved away from the tag to generate the separation. The tag frequency (b), linewidth (c), and absorption (d) are shown as a function of separation from the packaging. In (b) to (d) the open black squares correspond to the data in (a) that was acquired for the tag surrounded only by air, while open red circles correspond to the case when a high permeability ferrite was placed on the tag between the tag and the packaging.

Analytical model

The frequency of the tag may be predicted using a simple analytical model based on the geometry of the ferrite-filled foil cavity and the number *n* of additional dielectric-foil wraps. Since the total area, and therefore capacitance, of the additional wraps is approximately proportional to *n*, the frequency changes in accordance with that expected of an *LC* resonator with frequency given by

$$f = \frac{1}{2\pi\sqrt{LC_n}}\frac{1}{\sqrt{n}}, \qquad \text{Equation (1)}$$

where C_n is the capacitance per additional wrap. The inductance of the cavity is estimated by treating it as a parallel plate waveguide [13] since the cavity length l is much greater than its thickness t, *i.e.* $l >> t$. The magnetic field is assumed to be spatially uniform within the cavity, and parallel to both the plane of the cavity and to its width w_c. By considering an Ampèrian loop with one arm inside and one arm outside the cavity (perpendicular to the uniform current flow along the plate length l) the inductance of the cavity is [13]

$$L = \frac{\mu_0 \mu_r l t}{w_c}, \qquad \text{Equation (2)}$$

where μ_0 and μ_r are the permeability of free space and the relative permeability of the ferrite material respectively, and the smaller inductance due to the dielectric-filled section is neglected.

The capacitance may be estimated from the approximate total area of the additional wraps and the thickness of the dielectric film and is given by

$$C_n = \frac{2\varepsilon_0 \varepsilon_r n w_c (l+t)}{d}, \qquad \text{Equation (3)}$$

where ε_0, ε_r, are the permittivity of free space and the relative permittivity of the dielectric, $2w_c(l+t)$ is the approximate area of each additional wrap (see Figure 2(c)), d is the thickness of the dielectric, and the smaller capacitance of the ferrite-filled section is neglected. Assuming that there are no air gaps present between the dielectric film and the metal foil, the frequency of the tag

$$f = \frac{1}{2\pi}\sqrt{\frac{d}{2\varepsilon_0 \varepsilon_r \mu_0 \mu_r n l t (l+t)}}, \qquad \text{Equation (4)}$$

is then seen to be independent of the cavity width w_c within the model. The relative permittivity of the dielectric film (Melinex) is assumed to have a frequency independent value of 3.[14] The inductance of the tag in equation (2) may be rewritten as

$$L = \frac{d}{8\pi^2 \varepsilon_0 \varepsilon_r \xi^2 (l+t) w_c}, \qquad \text{Equation (5)}$$

where $\xi = f\sqrt{n}$. Equation 5 therefore allows the inductance of the tag to be determined without the need to determine the relative permeability.

Results and Discussion

The resonant frequency of the cavity is dependent on the cross-sectional area of the inductive foil loop and the permeability of the ferrite filling material. In practice there is also a weaker dependence on the cavity width [1]. The frequency of the tag can be further tuned via the number of additional capacitive dielectric/foil wraps. Starting with n = 10 wraps, the wraps were then cut away from the tag in 0.5 wrap steps and the resonant frequency recorded. In this study, the dimensions of the ferrite core (see Figure 1(c)) were l = 50 mm, w_f = 30 mm, and t = 1.3 mm. The width of both the foil cavity and subsequent dielectric/foil wraps was $w_c = w_f =$

30 mm, i.e. the cavity, wraps, and ferrite core had the same nominal width. The thicknesses of the metal foil and dielectric film were 50 μm and d = 25 μm respectively. For this geometry, Equation 3 yields a capacitance of $C_1 \approx 3.3$ nF for a single (n = 1) wrap. Figure 4(a) shows typical absorption spectra (grey spectra) acquired for a tag with n complete additional wraps for n = 1, 2, 3, 4. Fitted Lorentzian peaks are overlaid (black line). A background spectrum with a weak frequency dependence (not shown) was acquired and subtracted from each tag spectrum before peak fitting. The resulting spectra shown in Figure 2(a) are offset by 0.1 dB for clarity.

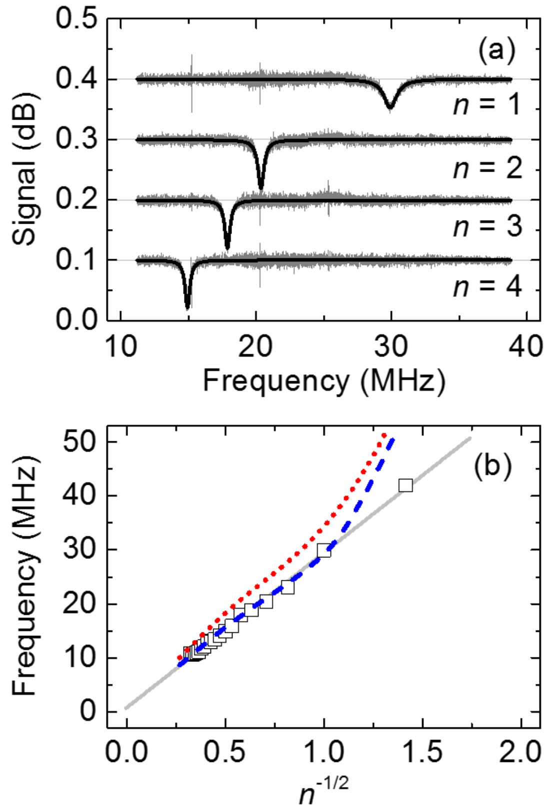

Figure 4. (a) The absorption spectra of tags with additional number of wraps n = 1, 2, 3, and 4. The measured spectra (light grey) are overlaid by fitted Lorentzian peaks from which the frequency, linewidth, and absorption are extracted. The spectra are offset by 0.1 dB for clarity. (b) The extracted frequencies of tags with n = 0.5 to 9.5. The linear fit as a function of $n^{-1/2}$ confirms that the additional wraps add capacitance, but do not significantly affect the inductance. The modelled curves (overlaid red and blue) show the frequencies calculated from the geometry of the tags and the ferrite permeability obtained from the manufacturer (blue dashed curve) and from permeammeter measurements [2] (red dotted curve).

As the number of wraps was decreased from 4 to 1, the frequency rapidly increased by a factor of 2 from 15 MHz to 30 MHz, in accordance with a $n^{-1/2}$ dependence. As the number of wraps was increased the frequency approached ~10.5 MHz, outside of the detection range for EAS at 8.2 MHz. The linear fit of Figure 4(b) confirmed the $n^{-1/2}$ frequency dependence of the tag. The linear dependence of frequency on $n^{-1/2}$ indicates that the frequency is tuned primarily by the change in capacitance of the tag with each additional wrap. This suggests that the ferrite-filled part of the cavity provides practically all of the tag inductance. The self-inductance of the additional wraps makes little contribution since both t and μ_r (in Equation 2) are approximately two orders of magnitude smaller in the wrapped part of the cavity compared to their values in the ferrite-filled part.

The analytical model (Equation 4) can be used to model the experimental data with each additional layer being assumed to have the capacitance given by Equation 3. The frequency dependence of the real part of the complex permeability of the ferrite was also included. The permeability data was obtained from the manufacturer, but was also extracted from permeammeter measurements performed on rectangular blocks, similar to those described in reference [15]. The modeled dependence of the tag frequency on $n^{-1/2}$ using the permeability data from the manufacturer and the permeammeter are shown as blue dashed and red dotted curves respectively. The curves were calculated by solving Equation 4 for n since the frequency dependent real part of the permeability is known. The model that assumed the manufacturer's permeability data is in good agreement with the experimental data for $n \geq 1$. However, when $n < 1$, *i.e.* a half wrap, the model predicts a significantly larger frequency than is observed in the experiment. A similar upturn in frequency is also predicted by the model that assumes the permeability values acquired from the permeammeter. The upturn could be attributed to an underestimate of either the capacitance or inductance of the tag when the first additional wrap is incomplete. The difference between the experimental data and the modeled data calculated using the real part of the permeability extracted from permeammeter measurements is observed over the entire range of n, in Figure 3(b). This is due to the known underestimate of the permeability, due to small air gaps where the RF magnetic flux is high in the permeammeter, which reduces the effective permeability obtained in this measurement. In contrast the manufacturer's values are obtained from toroidal specimens for which air gaps are eliminated.

The microwave absorption and spectral linewidth of the tag are also sensitive to the cavity dimensions and the number of additional wraps. The amplitude of the microwave absorption is proportional to the cross-sectional area of the ferrite-filled cavity. However, the absorption and linewidth are also sensitive to the frequency dependent loss associated with the ferrite filling material. For example, Figure 4(a) shows that higher frequency tags with a single wrap (n = 1) exhibit enhanced linewidth and reduced amplitude in contrast to lower frequency tags with (n = 2, 3, and 4). Figure 5(a) summarizes the frequency dependence of the resonance linewidth and quality factor (Q-factor = frequency/linewidth) of the tags as n is reduced from

9.5 to 0.5 in half-wrap increments. Between 10 MHz and 42 MHz the linewidth increases by approximately one order of magnitude, while at 42 MHz the *Q*-factor decreases to approximately one third of its peak value observed at ~20 MHz.

The ferrite filling material is required to have a large real part of the permeability (Re(μ_r)) and low magnetic loss (Im(μ_r)) in order to yield a tag with low frequency and high Q resonances. However, for the dielectric thickness of 25 μm and the range of *n* used for the prototype tags, the resonance frequency of the tags exceeds that at which it can be assumed that the real part is constant, and the imaginary part is small. The frequency dependence of the linewidth and *Q*-factor can then be understood from the dispersion of the

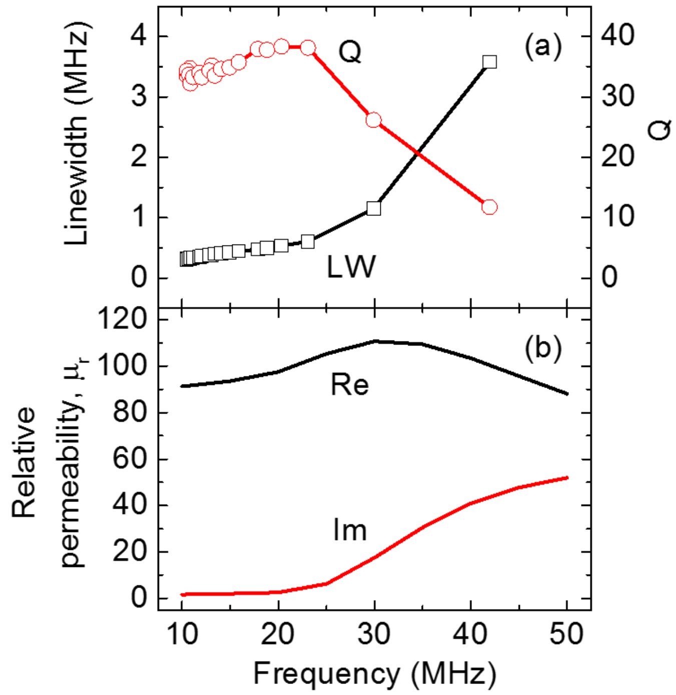

Figure 5. (a) The linewidth (LW) and Q-factor extracted from the measured absorption spectra for tags with number of turns, $n = 0.5$ to 9.5, plotted as a function of frequency. (b) The real and imaginary components of the complex permeability extracted from permeammeter measurements of the F16 ferrite filling material as a function of frequency. The peak in Re(μ_r) is seen to coincide with the increase of Im(μ_r). The increase of Im(μ_r) also coincides with the enhanced linewidth and reduced *Q*-factor in (a), indicating that magnetic losses in the ferrite core of the tag become significant above 25 MHz.

permeability μ_r of the ferrite filling material (Figure 5(b)), determined from the permeammeter measurements. The frequency dependence of Re(μ_r) and Im(μ_r) has the typical character described by Snoek [16, 17]. The measured value of Re(μ_r) at 10 MHz is ~90 and is sufficient to realize a tag with size and frequency required for EAS at 8.2 MHz. With increasing frequency, the value of Re(μ_r) increases to a peak of ~110 at 35 MHz, Figure 5(a), before falling. In contrast the value of Im(μ_r) at 10 MHz determined from the permeammeter measurements is ~1 and remains small until the frequency increases to ~20 MHz after which it increases to a peak value ~55 at 65 MHz, Figure 5(a). It is clear from Figure 5(a) and Figure 5(b) that the increase in linewidth and decrease in Q-factor are correlated with the increase in the imaginary component of the ferrite permeability corresponding to magnetic losses [3,4]. An increasing number of wraps ($n > 2$) allows the frequency of the tag to be tuned into the low loss regime where Re(μ_r) is large. Such tunability is essential to achieve the frequency, Q-factor, and signal amplitude required for detection by EAS gate systems. At the same time, the increased inductance of the ferrite-filled tag allows the lateral dimensions of the tag to be reduced to 3×5 cm^2: a small reduction in area compared to label tags that have adopted a standard size of 4×4 cm^2 [5].

To further confirm that the ferrite-filled section of the cavity provides the dominant contribution to the self-inductance of the structure, ceramic capacitors were electrically connected to the open end of only the ferrite filled part of the cavity. The range of capacitance of the ceramic capacitors ($1 < C < 7$ nF) was chosen to be similar to that calculated for two wraps of dielectric and foil. In accordance with equation 1, a linear fit of frequency, f versus $(nC_n)^{-1/2}$ (not shown) allowed a cavity inductance of 42.4 nH to be calculated. Here C_n and n can be considered as the capacitance of each ceramic capacitor and the number of capacitors added, respectively. A similar analysis can be applied to the wrapped tag. However, it is necessary to estimate the capacitance of each wrap from its geometry. The gradient ξ of the linear fit to f versus $n^{-1/2}$ in Figure 4(b) allowed the inductance to be estimated using Equation 5. The inductance of the wrapped tag was calculated to be 9.4 nH, slightly less than 1/4 of that determined for the cavity by using ceramic capacitors, and so the additional wraps do not appear to enhance the inductance. Instead this suggests that the model based on the geometry of the wraps overestimates the value of the total capacitance. This is associated with imperfect wrapping of the separate metal foil and dielectric film, leading to small gaps between the metal and dielectric that fill with air with relative permittivity $\varepsilon_r \sim 1$. Indeed, compressing the tag firmly between fingers was found to yield a further decrease in frequency consistent with enhancement of the capacitance through local removal of air gaps. To consistently minimize the influence of air gaps a firm tension was applied to the additional foil/dielectric warps while wrapping. The capacitance of two parallel plates, separated by a layer of dielectric of thickness d and relative permittivity ε_r, and air gap of thickness d_g, can be written as

$$C = \frac{\varepsilon_0 A}{\left(d_g + \frac{d}{\varepsilon_r}\right)}, \qquad \text{Equation (6)}$$

where A is the area of the capacitor. Therefore, an air gap with thickness equal to the dielectric thickness ($d_g = d$) reduces the capacitance by a factor $\left(\varepsilon_r \frac{d_g}{d} + 1\right)^{-1}$. If $\varepsilon_r = 3$, the capacitance may be reduced by a factor of 1/4 if $d_g = d$. The resulting overestimate of the wrap capacitance then leads to an underestimate of the inductance. Despite the best efforts to eliminate air gaps between the separate dielectric film and metal foil, their presence could be seen and a gap thickness of ~ d seems very reasonable. Therefore, the presence of air gaps is the most plausible explanation for the observed discrepancy in the tag inductance. In demonstration tags for retail trials discussed later in this article, the consistency of tag manufacture was improved by vacuum sealing the tags to remove all air gaps. However, for the present study of the tag response as a function of the number of turns it was not practical to vacuum seal the tag for each half wrap increment.

Finite element modelling

In order to gain further insight into the electromagnetic field distribution within the tag, finite element method (FEM) modeling was used to understand the current distribution in the foil of the cavity and additional wraps. The previously stated dimensions of the ferrite core length and thickness, foil and dielectric thickness, and number of additional wraps were assumed, while the frequency dependent complex permeability values obtained from the permeammeter measurements were used. The model assumed an infinitely wide cavity, *i.e.* $w_f = w_c \rightarrow \infty$. In a simplified approach, the metal foil was assumed to be a perfect electrical conductor (PEC) and eigenmode solutions of the quarter-wavelength TEM mode were obtained for a tag with number of wraps $n = 1$ and $n = 2$. Meshing within the microscale thickness of the foil and dielectric is computationally challenging due to the centimeter length scale of the cavity. If the metal is not treated as a PEC then meshing within the metal foil, to account for the skin depth, can lead to a reduction of the resonance frequency of a cavity TEM mode [18]. Figure 6 shows *x*-*y* cross-sections of the electromagnetic field distributions taken across the width and midway along the length of a tag with number of wraps $n = 1$. For clarity, the field distributions are only shown at ±1 mm from the center of the tag (i.e., from $l/2$) along *y*. The current direction and density are represented by black arrows on the surfaces of the PEC foil.

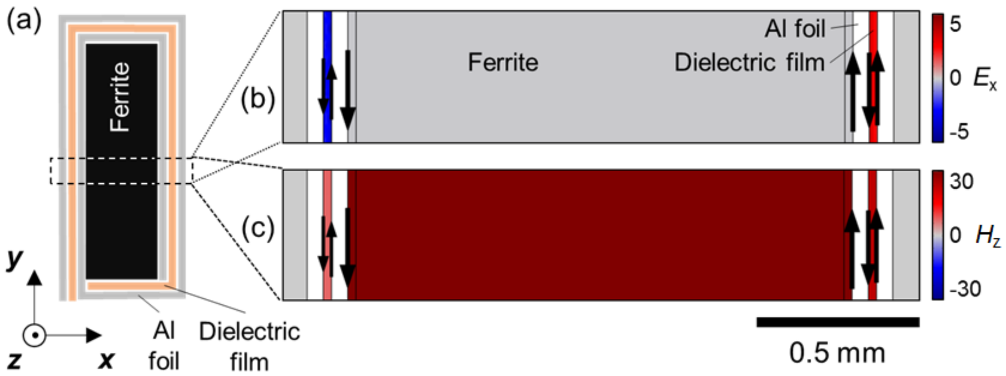

Figure 6. Finite element modelling (FEM) of tags for $n = 1$ and modelled frequency of 4.57 MHz. Plots in (b) and (c) have been extracted from a finite width cross-section in the *xy* plane close to the center of the tag length, as indicated in the schematic in (a), not to scale. In (b) the amplitude of the *x*-component of the electric field is shown in accordance with the color scale (in Vm^{-1}). Regions of large electric field amplitude are confirmed to lie within the thin dielectric film of the capacitive wraps. In (c) the amplitude of the *z*-component of the magnetic field is shown in accordance with the color scale (in A/m). Regions of large magnetic field are confirmed to lie within the ferrite core, but are also found within the dielectric of the additional wraps. In (b) and (c) the direction and density of current on the surface of the PEC is indicated by the direction and length of the arrows.

The decrease in frequency of the modelled tag when *n* is increased from 1 to 2 wraps is in agreement with the experiment. However, the values of the modeled frequencies (4.57 MHz for $n = 1$, and 3.77 MHz for $n = 2$) do not agree with those of the experiment (~30 MHz for $n = 1$, and ~20 MHz for $n = 2$). The discrepancy is expected and is due to the assumption of an infinitely wide cavity [9]. For a cavity of infinite width, the magnetic field generated by the electric current distribution is confined to the ferrite core with large relative permeability. However, for a cavity of finite width, the magnetic field also extends outside the core into free space surrounding the cavity where the relative permeability is unity. The volume averaged permeability, seen by the internal magnetic field within the core and the stray field outside the tag, is significantly reduced with respect to the permeability of the ferrite, leading to a reduction of the self-inductance, and therefore a higher frequency as observed in the experiments.

Despite the quantitative discrepancy, the model indicates that the current flows in opposite directions on successive dielectric/foil interfaces of the wrapped cavity structure. The current flow on the surfaces of the wrapped metal foil is readily understood from the unwrapped picture of the cavity in Figure 1(a) where current in the foil on opposite sides of the dielectric flows in opposite directions. A magnetic field antinode is observed where maximum current flow occurs, in accordance with Ampère's law (Figure 6(c)). Figure 6(b) confirms that the amplitude of the E_x component is largest in the capacitive part of the cavity where the foil is separated by the thin dielectric film, and in fact is maximum at the open end of the cavity, neglecting fringing effects [9]. Since the capacitive part of the cavity is wrapped around the core, the sign of E_x is opposite on opposite sides of the cavity, as indicated by red and blue E_x contrast in Figure 6(b). A movie of the alternating current and field distributions is provided in the Supplementary Material for a tag with modified dimensions for the purposes of demonstration. Further experimental and FEM investigations are now required to understand the current distribution within metal foils with thickness comparable to the skin depth.

Profiles of the *z*-component of magnetic field within the ferrite (shaded yellow) and the dielectric regions of the animated tag[19] are shown Figure 7(a). The profiles were extracted along the dashed line section A-A' in Figure 7(b). The profiles indicate a linear decrease of the magnetic field amplitude along the length of the dielectric filled section, but almost constant amplitude within the ferrite. In contrast the electric field amplitude is approximately constant within the dielectric-filled section before decreasing monotonically into the ferrite-filled section.

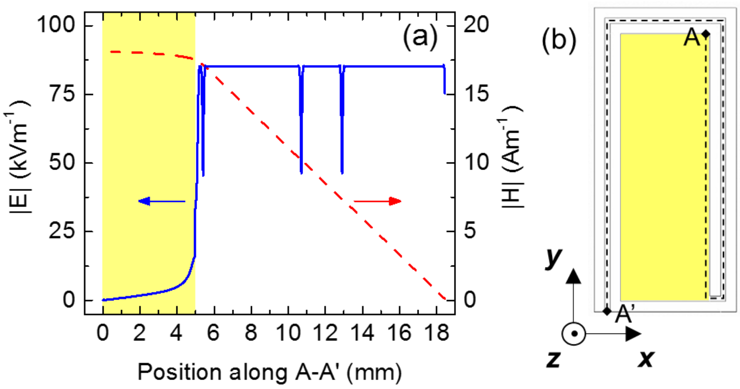

Figure 7. (a) The time-averaged magnitude of the electric field (blue solid curve) and magnetic field (red dashed curve) are shown as a function of position along the length of the tag cavity, extracted from the dashed line section A-A' in (b). The section passes along the length of the ferrite filled part of the cavity (0 to 5 mm shaded yellow in (a) and (b)) before wrapping around into the dielectric filled part of the cavity. The profiles are extracted from the modelled animation in the supplementary material.

Prototype EAS tags

While the tags considered so far have allowed the underlying physics to be understood, their resonance frequency was consistently too high for EAS applications. Furthermore, the *Q*-factor and signal amplitude compare unfavorably with those of existing EAS tags, and do not provide the signal quality required to trigger an EAS gate system. To reduce the frequency to 8.2 MHz it is necessary to increase the capacitance by reducing the dielectric thickness and eliminating air gaps where possible. At the same time the *Q*-factor and signal strength can be enhanced by reducing the cavity width with respect to that of the ferrite core, i.e. making $w_c < w_f$, in accordance with previous work [9].

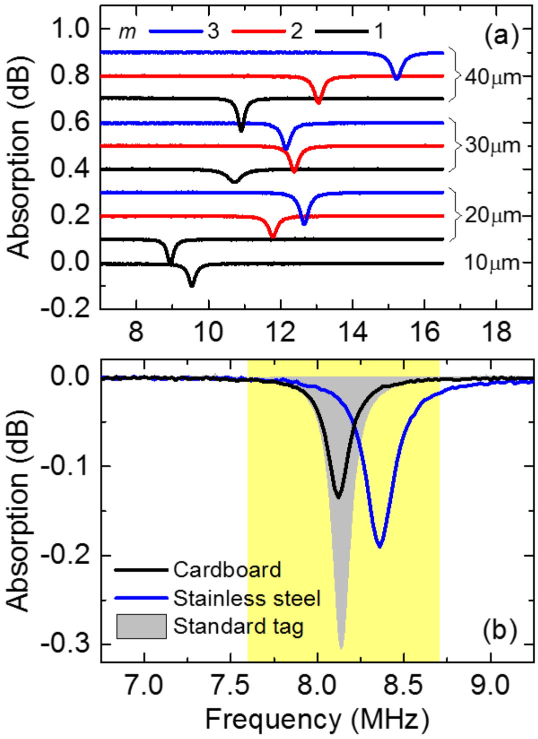

Figure 8. (a) Measured absorption spectra for tags with n = 1 constructed with 40 μm, 30 μm, and 20 μm foil thickness with triple (m = 3), double (m = 2), and single (m = 1) layer applications of heat-seal lacquer (black, red, and blue curves respectively). Only a single layer of lacquer was applied to the 10 μm thick foil. (b) Measured absorption spectra for a proof of concept wrapped tag with n = 2 when placed on stainless steel (blue curve) and cardboard (black curve) packaging. The spectrum for an EAS industry standard 40 × 40 mm^2 label tag is shown (shaded grey) in addition to the frequency band of EAS detection gates (shaded yellow).

To enhance the capacitance a vinyl-based heat-seal lacquer was used as the dielectric layer. While the precise composition was unknown, heat-seal lacquers typically contain polyvinyl-chloride (PVC), which has a dielectric constant of ~3.4 and is similar to that of the PET film used so far. Single (m = 1), double (m = 2), and tri-layers (m = 3) of lacquer were rolled onto foils of thickness 40 μm, 30 μm, and 20 μm. For a foil thickness of 10 μm, only a single layer of lacquer was applied. One advantage of laminating one side of the foil with lacquer is the elimination of air gaps between one of the two dielectric/foil interfaces within the capacitive part of the tag.

Tags with foil/lacquer laminates were made using an F16 ferrite core with l = 48 mm, w_f = 30 mm, and t = 1.5 mm (a slightly shorter and thicker core than used previously). Each laminate strip was wrapped around the core to form the cavity and only one complete wrap. The width of the strip lacquer and foil are necessarily equal. Electrical contact between the cavity and the single additional wrap at the edges of a strip of uniform width can short circuit the capacitive wrap. To prevent this, laminate strips initially 30 cm long, were tapered from approximately 2 cm wide at one end, to 1 cm wide at the other. This ensured that the lacquer provided electrical isolation of the foil edges of the ferrite-filled part of the cavity from those of the wrapped part of the cavity.

The absorption spectra for tags made with laminate strips of different foil and lacquer thickness are shown in Figure 8(a). In general the tag frequency decreased as the lacquer thickness was reduced. This is clear for a foil thickness of 20 μm and 40 μm, but for the 30 μm thick foil the decrease was non-monotonic and ascribed to imperfect reproducibility of cutting and wrapping of the laminate by hand. The tag frequency can also be seen to decrease as the metal foil thickness was reduced. This is most clearly observed for two layers of lacquer ($m = 2$), while triple and single layers of lacquer showed slight deviations from this trend. The reduction in frequency for tri-, double, and single layers of lacquer was most significant for tags with a laminate foil thickness of 40 μm. The measured tag frequencies were used to estimate the lacquer thickness, (equation 4) by comparing the frequency of a tag with one additional wrap ($n = 1$) of foil(40 μm)/lacquer laminate to that of such a tag constructed with one additional wrap of separate metal foil and dielectric film, see Figure 2(a). It was assumed that the dielectric constant of PET and PVC were ~3 and ~3.4 respectively. Differences in the ferrite core dimensions were accounted for, in addition to the different value of the core permeability at the different tag frequencies. The thickness of a single, double, and tri-layer of heat-seal vinyl lacquer was estimated to be 3.4 μm, 4.9 μm, and 6.6 μm respectively.

The irregular change in frequency with decreasing lacquer thickness for the 30 μm foils, and for decreasing metal thickness for the single and triple layer lacquer, is ascribed to the difficulty of hand-wrapping thin laminates, i.e., ensuring that the wrap is tight while avoiding damage to the thin dielectric lacquer, foil, or both. Air gaps between the exposed surfaces of the lacquer and the foil of the cavity could not be eliminated completely and are known to affect the observed frequencies by reducing the capacitance of the wrap.

The most effective reduction of frequency to a value close to 8.2 MHz was achieved using 20 μm and 10 μm thick foils and a single layer of lacquer for which tag frequencies of ~8.94 MHz and 9.54 MHz were achieved respectively. The slightly higher tag frequency achieved with the 10 μm thick foil was again ascribed to air gaps, since this delicate laminate could not be wrapped tightly. To assist with the elimination of such air gaps, the tag was vacuum secured by heat-sealing inside a plastic pocket. This allowed the capacitance to be optimized and the frequency reduced to below 8.2 MHz. A small amount of air was then allowed back into the bag via a small puncture hole to reduce the capacitance and increase the tag frequency. This process was carried out with the tag placed onto stainless steel packaging, while the frequency of the tag was monitored *in-situ* as the air flowed back between the cavity and the single additional wrap to achieve a frequency close to 8.2 MHz, Figure 8(b) blue curve. The puncture was then sealed with adhesive tape and the vacuum pocket heat sealed again to prevent the puncture from leaking further. The tag frequency was 8.36 MHz, slightly higher than the preferred 8.2 MHz. However, the EAS gate systems have a detection frequency band from 7.6 MHz to 8.7 MHz (Figure 8(b), yellow band). In fact, when the tag was placed on non-metallic packaging such as cardboard, the detuning from 8.36 MHz to 8.12 MHz (Figure 8(b) black curve) was sufficiently small that the tag frequency remained within the detection band of the gate[20]

To assess the viability of the wrapped planar tag as an EAS solution for metallic packaging it should perform to a similar standard to existing EAS tags. For comparison, the spectrum of the standard EAS label tag, with frequency of 8.14 MHz measured in free space, is also shown in Figure 8(b), shaded grey. The wrapped planar cavity tag exhibited reduced absorption, increased linewidth, and reduced *Q*-factor, with respect to the standard tag, Table 1. To prevent the linewidth from becoming too large, particularly for packaging containing ferrous material, the wrapped planar tags were integrated with an Al foil shield. The shield had a thickness of at least one skin depth (~30 μm) at 8.2 MHz and an area of ~50 × 50 mm^2 and could either be contained within the heat-sealed vacuum pocket, or attached with adhesive to the outside of the pocket. The shield helps to prevent magnetic losses within ferrous metallic packaging, e.g., magnetization reorientation and domain wall motion, driven by the RF magnetic field associated with the tag.

	Wrapped tag		Standard tag
	Stainless steel	Cardboard	Air
Frequency (MHz)	8.36	8.12	8.14
Linewidth (MHz)	0.19	0.15	0.12
Q-factor	43	54	66
Peak absorption (dB)	-0.19	-0.13	-0.31
Read distance (cm)	80	80	90

Table 1. Wrapped tag characteristics extracted from measured absorption spectra of Figure 8(b) for a vacuum sealed, proof of concept wrapped tag with $n = 2$ when placed on stainless steel and cardboard packaging. The characteristics for an EAS industry standard 40×40 mm^2 label tag are also shown.

The cross-sectional area of the planar spiral inductor coil of the standard tag (~1600 mm^2) exceeds that of the inductive part of the wrapped tag (~72 mm^2) by more than 20 times. Despite this, the enhanced inductance of the cavity, due to the high Re(μ_r) ferrite core, leads to an absorption that is ~40% to ~60% that of the standard tag absorption, which allows the wrapped tag to effectively couple to the EAS detection gate. Furthermore, the absorption of the wrapped tag was enhanced when the tag was placed on stainless steel instead of cardboard. One tentative explanation is that the in-plane component of the RF magnetic field generated by the EAS detection gate is enhanced in the vicinity of metallic packaging, which helps it to couple to the tag.

To confirm the reproducibility and assess the viability of the hand-made wrapped tags, a small batch were made in anticipation of retail trials. To enhance the coupling to EAS detection gates the ferrite core thickness was increased to 3 mm. Laminate strips with composition Al(18 μm)/vinyl lacquer(3 g/m^2) were cut by Multifoil Ltd.[1] in reproducible batches. The strips had initial length of 30 cm, and were tapered from 2 cm at one end, to 1 cm at the other. Of 45 tags constructed and vacuum sealed in the way described previously, 37 tags exhibited frequencies between 8 MHz and 8.4 MHz at the end of their construction. Figure 9 shows exemplar absorption

[1] 24 Marsh Green Road West, Marsh Barton, Exeter, EX2 8LZ

spectra acquired during the construction of a tag. Initially, the heat-sealed vacuum enclosure reduced the tag frequency to 5.5 MHz in free space, and 6.8 MHz on stainless steel as the air is removed from the capacitive part of the tag.

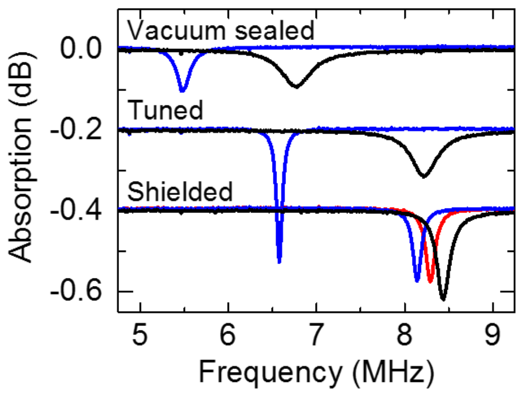

Figure 9. Absorption spectra measured during the construction of a wrapped tag for retail trial. Spectra acquired for the tag in free space, and on stainless steel packaging, are shown as blue and black curves respectively. The spectrum for the EAS industry standard 40 × 40 mm^2 label tag is also shown (red curve). Note that the label tag is not shielded, but shown for comparison only. The top two 'vacuum sealed' spectra were acquired after the ferrite and wrapped foil/lacquer laminate strip were heat-sealed in a vacuum pocket. The middle two 'tuned' spectra were acquired after the vacuum was punctured, the tag tuned to ~8.2 MHz on stainless steel packaging, and then heat sealed once again. The bottom 'shielded' spectra were acquired after a 50 × 50 mm^2, 50 μm thick, Al foil shield was attached to the packaging side of the tag.

Once the tag was tuned to approximately 8.2 MHz on stainless steel, there is a significant difference between the tag frequency on stainless steel (8.2 MHz) and in free space (6.6 MHz). The addition of an Al foil shield to one side of the tag permanently mimics the presence of non-ferrous metallic packaging so that the tag frequency in free space (8.1 MHz) and on non-magnetic stainless steel (8.4 MHz) are more similar to each other, are both within the detection frequency band of EAS gates, and both similar to the industry standard EAS 40 mm label tag (8.3 MHz in Figure 9). When the wrapped tag is placed onto metal packaging its absorption exceeds that of the label tag in free space, demonstrating that it makes more effective use of the ferrite block, than simply placing the label tag onto the ferrite, as shown in Figure 3(d).

	Mean	Standard deviation	Minimum	Maximum
Frequency (MHz)	8.16	0.0760	8.01	8.28
Linewidth (MHz)	0.211	0.0552	0.116	0.296
Q-factor	41.8	12.6	27.3	69.9
Peak absorption (dB)	-0.151	0.0458	-0.241	-0.0923
Read distance* (cm)	83.3	7.76	70.0	90.0

Table 2. Average wrapped tag characteristics extracted from measured absorption spectra for 37 vacuum sealed, proof of concept wrapped tags with $n = 2$ when placed on stainless steel packaging.

*For 35 of 37 tags only, measured along the center-to-center line of an EAS security gate to the position at which a tag triggers the gate.

The mean frequency, linewidth, Q-factor, peak absorption, and read distance are provided in Table 2, in addition to their standard deviation and minimum and maximum values. The good reproducibility of this small batch of tags demonstrates that there is potential for larger scale manufacture of the wrapped tags for EAS solutions for metallic packaging. Of particular note is the narrow range of frequencies that lie well within the EAS detection range, and the variation in read distance, which approaches the desired distance for EAS detectors placed to either side of the exit within a retail store.

Summary

In summary, planar quarter-wavelength cavities have been adapted to develop an EAS tag solution for metallic packaging. The tag can be described as a quarter-wavelength cavity with an impedance mismatch part-way along its length, between a section containing a high permeability ferrite filling material, and another section containing a thin dielectric filling material. Alternatively, the same two sections can be thought of as contributing the lumped inductance and capacitance, respectively, of an LC-resonator. These models of the tag have allowed the current distribution flowing through the wrapped foil, and the inductive and capacitive contributions to the impedance to be understood. This understanding has allowed working prototypes to be demonstrated in small batches with well-reproduced characteristics such as frequency and linewidth, which make them viable solutions to the problem of tagging metallic packaging within the EAS industry.

Acknowledgements

The authors gratefully acknowledge the financial support of the UK Engineering and Physical Sciences Research Council via grants EP/L015331/1 (Centre for Doctoral Training in Metamaterials, E.G.), EP/I500219/1 (A planar microwave cavity loaded with ferrromagnetic material: a new 8.2 MHz anti-theft tag for metallic packaging within the retail sector), and EP/R004781/1 (EPSRC and QinetiQ Ltd. via the TEAM-A prosperity partnership, I.R.H.). The authors make special thanks to Andy Hayling of MagDev Ltd. for the provision of custom ferrite cores, and Mike Cochran of Crown Packaging PLC. for the provision of prototype aluminum foil/vinyl lacquer laminates.

Open access to supporting research data is provided by Open Research Exeter at http://hdl.handle.net

References

1. Liberal, I., A.M. Mahmoud, and N. Engheta, *Geometry-invariant resonant cavities.* Nature Communications, 2016. **7**: p. 10989.
2. Gold, S.H. and G.S. Nusinovich, *Review of high-power microwave source research.* Review of Scientific Instruments, 1997. **68**(11): p. 3945-3974.
3. Stern, I., et al., *Cavity design for high-frequency axion dark matter detectors.* Review of Scientific Instruments, 2015. **86**(12): p. 123305.
4. Alici, K.B., et al., *Experimental verification of metamaterial based subwavelength microwave absorbers.* Journal of Applied Physics, 2010. **108**(8): p. 083113.
5. R. E. Collin, Field Theory of Guided Waves, 2nd ed. (Wiley-IEEE Press, 1990).
6. Porto, J.A., F.J. García-Vidal, and J.B. Pendry, *Transmission Resonances on Metallic Gratings with Very Narrow Slits.* Physical Review Letters, 1999. **83**(14): p. 2845-2848.

7. Sievenpiper, D., et al., *High-impedance electromagnetic surfaces with a forbidden frequency band.* Microwave Theory and Techniques, IEEE Transactions on, 1999. **47**(11): p. 2059.
8. Zhao, B. and Z.M. Zhang, *Study of magnetic polaritons in deep gratings for thermal emission control.* Journal of Quantitative Spectroscopy and Radiative Transfer, 2014. **135**: p. 81-89.
9. Keatley, P.S., et al., *Ferrite-filled cavities for compact planar resonators.* Applied Physics Letters, 2014. **104**(2): p. 022405.
10. H. Imaichi; T. Matsumoto; Y. Suzuki; K. Himura; T. Haneda, *Resonant tag and method of manufacturing the same*, United States Patent 5,447,779 (1995).
11. Acher, O., P*ermeability enhancement of soft magnetic films through metamaterial structures.* Journal of Magnetism and Magnetic Materials, 2008. 3**20(**23): p. 3276-3281.
12. Lockyear, M.J., A.P. Hibbins, and J.R. Sambles, T*ransmission of microwaves through a stepped subwavelength slit.* Applied Physics Letters, 2007. 9**1(**25): p. 251106.
13. Ramo, S., Whinnery, J.R. and van Duzer, T. (1994) Fields and Waves in Communication Electronics. John Wiley & Sons, Inc., New York.
14. Svorčík, V., et al., P*ermittivity of polyethylene and polyethyleneterephtalate.* Journal of Materials Science Letters, 2000. 1**9(**20): p. 1843-1845.
15. Barry, W., A *Broad-Band, Automated, Stripline Technique for the Simultaneous Measurement of Complex Permittivity and Permeability.* Microwave Theory and Techniques, IEEE Transactions on, 1986. 3**4(**1): p. 80-84.
16. Snoek, J.L., G*yromagnetic resonance in ferrites.* Nature, 1947. 1**60(**4055): p. 90-90.
17. Snoek, J.L., Dispersion and absorption in magnetic ferrites at frequencies above one MC/s. Physica, 1948. 1**4(**4): p. 207-217.
18. Suckling, J.R., et al., F*inite Conductance Governs the Resonance Transmission of Thin Metal Slits at Microwave Frequencies.* Physical Review Letters, 2004. 9**2(**14): p. 147401.
19. Supplementary Material
20. R.J. Hicken, P.S. Keatley, and A.P. Hibbins, *Radio frequency detectable device* International Patent Number WO2014/195678 (2014)